Controlled assembly of gold nanorods using tetrahydrofuran

ARTICLE *in* RSC ADVANCES · JANUARY 2013

Impact Factor: 3.84 · DOI: 10.1039/C2RA23300B

RSC Advances

RSC Publishing

PAPER

View Article Online
View Journal | View Issue

Controlled assembly of gold nanorods using tetrahydrofuran

Cite this: *RSC Advances*, 2013, **3**, 2690

Shanlin Ke, Caixia Kan, Jinsheng Liu and Bo Cong

Received 12th December 2012,
Accepted 17th December 2012

DOI: 10.1039/c2ra23300b

www.rsc.org/advances

One dimensional gold nanostructure is one of the most studied colloidal nanostructures due to its unique optical properties and promising applications. Compared with the study of isolated Au nanorods (AuNRs), researches on the controlled assembly of AuNRs in predictable structures and consequent coupling-induced wealthy changes in optical spectra remain challenging at present. In this paper, we present an effective method for assembling AuNRs in side-by-side and end-to-end modes through simply adding water-soluble organic solvents (such as tetrahydrofuran and 3-mercaptopropionic) to the as-prepared AuNRs colloid. These two assembly modes are controlled by the concentration of organic solvent. The longitudinal surface plasma resonance of AuNRs shows great coupling effect for these two assembly modes, blue-shifting during the side-by-side assembling and red-shifting with end-to-end assembling.

Introduction

Noble metal nanostructures exhibit rich optical properties resulting from the collective resonant oscillation of conduction electrons under the irradiation of light, so-called surface plasmon resonance (SPR).[1,2] Among the various shaped nanostructures, one dimensional Au nanostructure (such as nanorod) is one of the most studied colloidal nanostructures. Due to the anisotropic shape, Au nanorod displays two SPR bands corresponding to its width and length known as the transverse mode (SPR_T) and longitudinal mode (SPR_L). The SPR_T is located at $\sim$520 nm, while the SPR_L can be tuned in a large visible-near infrared (Vis-NIR) region, highly depending on surrounding medium, changes of surface charge density, aspect ratios, surface coating, and aggregation degree.[3–6] For their stability, low biological toxicity, bright color and unique optical properties, AuNRs have also been explored in great potential applications, such as five-dimensional optical recording-reading,[7] direct observation of chemical reactions,[8,9] nanoplasmonic probes for catalytic reactions,[10–12] and therapy in cancer research.[13–16]

With the development of controllable synthetic technology characterization of nanomaterials, nanoparticles can be assembled into desired arrangements, and the assembly exhibits collective properties different from those displayed by individual ones. Compared with the isolated Au nanorods (AuNRs), it is found that when two AuNRs placed in close proximities with a nanogap, near-field coupling between the surface plasmons of the neighbouring nanorods occurs owing to the transfer and confinement of electromagnetic energy, leading to a strong electric field enhancement of the local nanogap and wealthy changes in the optical spectra. For certain shaped AuNRs, the assembly mode is sensitive to the tip or side surface functionalization, and the SPR_L shows great sensitivity to slight changes of the assembly, such as arrangement morphology, the number of assembled rods, binding molecule, gap size, and, packing symmetry *et al.* This property can be converted into a bio- and chemical sensing modality, such as detection of transition metal ions,[17,18] toxins,[19] some elements,[20,21] and antigens.[22] Therefore, an increasing amount of attention has been directed toward the assembly of coupled AuNRs.

In recent years, significant progress has been made on developing methods for AuNRs assembly, such as binding rods to a surface by utilizing electrostatic interactions,[23,24] evaporation-induced assembly of nanorods into a close-packed superstructure (or onto the patterned substrate) without any additives,[25–28] polymer-composite driven organization,[29,30] and solution-phase assembly.[19,31,32] In these categories, solution-phase assembly could allow one to access different types of assemblies in a scalable fashion by changing the polarity of AuNRs solution or through adsorbing polar groups onto the surface of AuNRs.[29,32–34] A large number of reports have dealt with the end-to-end assembly of rods induced through tip selective bindings of proteins, thiolated polymers, small molecules.[32,35–40] Hydrogen-bonding between carboxylic acids was also suggested to be critical in acid-mediated assembly. Because the charge state and the hydrogen-bonding capabilities of an acid are pH-dependent, pH can be used to modulate the assembly of rods, as demonstrated by Sun and co-workers.[41]

College of Science, Nanjing University of Aeronautics and Astronautics, Nanjing 210016, P. R. China. E-mail: cxkan@nuaa.edu.cn

In this paper, we demonstrated a simple and effective technique for side-by-side and end-to-end assembly of AuNRs with a high-yield.

Experimental

Materials

Cetyltrimethylammonium bromide (CTAB, 99%, Nanjing Robiot Co. Ltd.), sodium tetrahydridoborate ($NaBH_4$, 99%, Sinopharm Chemical Reagent Co. Ltd.), and tetrachloroaurate ($HAuCl_4 \cdot H_2O$, 99.9%, Shanghai Chemical Reagent Co. Ltd.), sscorbic acid (AA, $\geqslant$99.7%, Sinopharm Chemical Reagent Co. Ltd.), 5-bromosalicylic acid (99%,Adamas reagent Ltd.), silver nitrate ($AgNO_3$, >99.8%, Sinopharm Chemical Reagent Co. Ltd.), 3-mercaptopropionic acid (MPA, >98%, TCI Shanghai), tetrahydrofuran (THF, Nanjing Chemical Reagent Co. Ltd.). All reagents were used without further purification. Water was purified using a Millipore-MilliQ setup for ultrapure water (18.25 M).

Synthesis of AuNRs

AuNRs were prepared by the seed-mediated method, as reported by Ye *et al.*[42]

Seed solution. The seed solution for AuNRs was prepared by adding $HAuCl_4$ (0.05 mL, 0.05 M) to an aqueous solution of CTAB (10 mL, 0.1 M). After stirring for 1 min, ice-cold $NaBH_4$ (0.6 mL, 0.01 M) was injected into the solution under vigorous stirring. The solution color changed from yellow to brownish-yellow. The seed solution was obtained after stirring for 2 min and aged at room temperature before usage. The as-obtained ultrafine seeds (with size of $\sim$3 nm) are very active indicated by the color change from brownish to red within one day.

Growth solution. For the preparation of growth solution, 0.912 g CTAB together with 0.228 g 5-bromosalicylic acid was dissolved in 49 mL water. Then $AgNO_3$ solution (0.24 mL, 0.02 M) was added under stirring, followed by addition of $HAuCl_4$ (0.5 mL, 0.05 M). After slow stirring for 15 min, AA solution (0.130 mL, 0.1 M) was added as a mild reducing agent. AA used in this synthesis is unable to reduce Au (III) to the metallic state, instead of Au(I) state, under the high CTAB concentration and low pH ($\sim$2.5) conditions, which accounts for the colorless reactant solution after adding AA.

AuNRs growth. After aging for different times (30–60 min), 0.06 mL of ''seed'' solution was added into the as-prepared growth solution. The resultant mixture was stirred for 30 s and left undisturbed at $\sim$30 °C for 12 h. The color of the reactant solution slowly changed from clear (slight brownish) to red (for AuNRs with aspect ratio $\sim$4), indicating the formation of AuNRs. Through adjusting experimental parameters, such as the amount of seed solution, the concentration of $AgNO_3$, the degrees of acidity, aspect ratios of the obtained AuNRs can be controlled.

The obtained products were purified by centrifuging at 2500 RPM for 5 min to remove the large sized nanoparticles deposited at the bottom. Then AuNRs were further purified by centrifuging at 13 500 RPM (25 min) for two times, leaving appropriate CTAB concentration to stabilize AuNRs colloid.

Assembly of AuNRs

The side-by-side assembly of AuNRs was carried out at room temperature by adding THF to the AuNRs colloid. Interestingly, different colors were observed when different amount of THF was added. Moreover, these colors changed immediately, indicating the assembly of the nanorods starts with the addition of THF. The end-to-end assembly of the AuNRs proceeded with addition of MPA to the colloids of isolated AuNRs and THF-induced side-by-side assembled AuNRs at pH >8. The assembly process was monitored by the evolution of absorption spectra.

Characterization

The absorption spectra of the prepared samples were collected on violet-visible-near infrared (UV-Vis-NIR) spectrometer (UV-6300) in the range of 200–1100 nm. The products were purified repeatedly with deionized water. Then, the samples were deposited on copper grids covered by an amorphous carbon film and HRTEM grids for further measurements. Microscopic observations and selected area electron diffraction (SAED) were carried out using transmission electron microscopy (TEM: JEOL-100CX) and high-resolution TEM (HRTEM: JEOL-2011).

Results and discussion

It is understood that CTAB molecules preferentially bind along the longitudinal sides of AuNRs, the ends deprived of protection and allowed for the binding of mercapto groups (–SH) to the ends facets.[34,43,44] Fig. 1A illustrates the stages for the formation of stable nanorod pairs *via* a destabilization and stabilization sequence. Fig. 1B shows the molecular structure of THF and MPA. THF is polar molecule, which is one of the strongest polar ethers, a good solvent for CTAB. CTAB bilayer along the sides of AuNRs imparts the electrostatic stability to colloid. When THF was injected to the CTAB-stabilized AuNRs colloid, CTAB solubility is increased, and the electrostatic

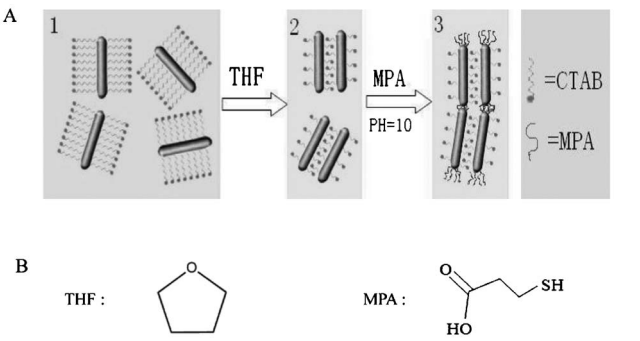

Fig. 1 Schematic diagram depicting the stages of the assembly of AuNRs (A), and molecular structure of THF and MPA (B). AuNRs are coated with a bilayer of CTAB along the side facets (1). The addition of THF to the AuNRs colloid increases CTAB solubility and induces the assembly of AuNRs in side-by-side orientations (2). End-to-end assembly of AuNRs pairs (3) can be achieved by addition MPA at pH = 10.

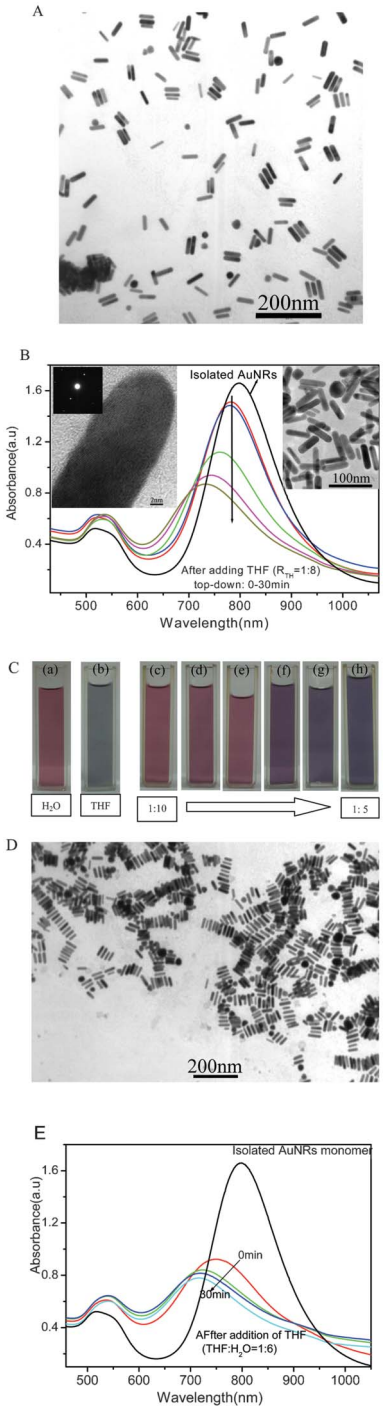

Fig. 2 (A) TEM image of the final product for the side-by-side assembled AuNRs with R_{TH} = 1 : 8. (B) Absorption spectra of AuNRs side-by-side assembled as a function of time with R_{TH} = 1 : 8, insets show TEM images of isolated AuNRs colloid, lattice spacing and SAED pattern; (C) colors of AuNRs colloids: isolated AuNRs dispersed in H_2O (a), concentrated AuNRs dispersed in THF (b), and addition of different amount of THF, (from (c) to (h) R_{TH} = 1 : 10,1 : 9,1 : 8,1 : 7,1 : 6,1 : 5); TEM image (D) and optical absorption spectra (E) of side-by-side assembled AuNRs with R_{TH} = 1 : 6.

stabilization of CTAB is reduced. The tunability of electrostatic repulsion and property altering (such as surface tension) of solvent enable controlled assembly of the colloidal particles.

With addition of THF to the AuNRs colloid, side-by-side assembly is driven by van der Waals attraction between the AuNRs and the steric repulsion at the ends of AuNRs (2). The numbers of dimer, trimer and polymer depend on the assembling time and amount of THF, as time progresses, colloid color changes obviously with increasing the amount of THF. MPA, a thiol reagent containing an –SH group, was used for the end functionalization of AuNRs. With the addition of MPA to isolated AuNRs or AuNRs pairs (2) at pH >8, end-to-end assembly of the AuNRs (or pairs) proceeds gradually (3).

Fig. 2A shows the representative TEM image of AuNRs assembled in side-by-side mode with R_{TH} = 1 : 8 (volume ratio THF : H_2O (R_{TH}) = 1 : 8). It can be seen that most of the AuNRs are assembled in dimer or trimer. Solution-phase organization could allow access to different types of assemblies. However, it may be difficult to determine whether a particular assembly truly occurred in solution or it arose from the solvent evaporation, since TEM technique generally requires a dried sample. Previous theoretical and experimental work suggested that side-by-side assembly of AuNRs leads to blue-shifting of

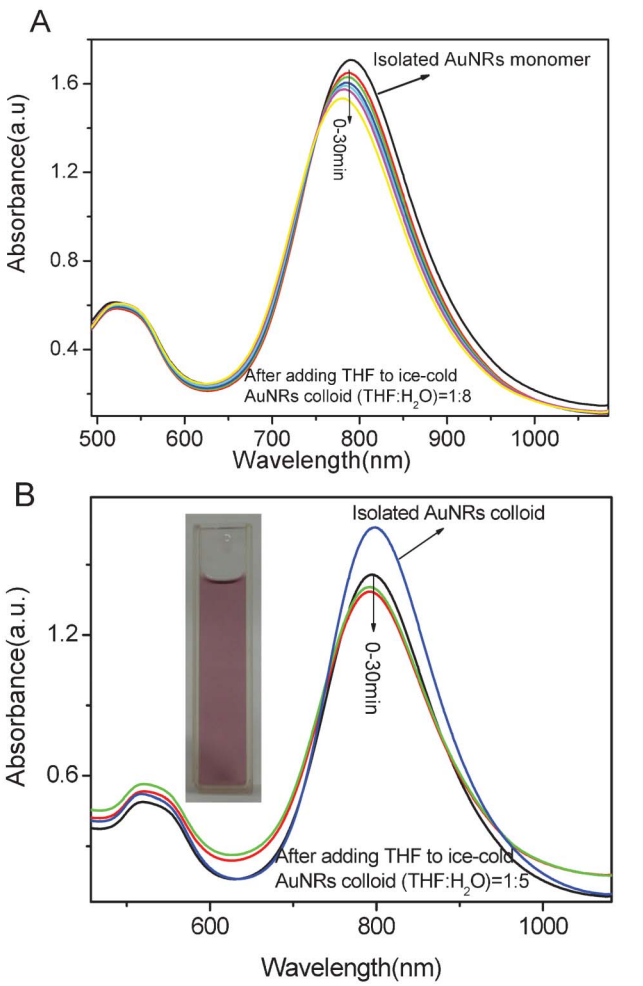

Fig. 3 Absorption spectra of ice-cold AuNRs after addition of THF with R_{TH} = 1 : 8 (A) and R_{TH} = 1 : 5 (B). Inset for the colloid photograph shows no obvious color change compared with that of isolated AuNRs.

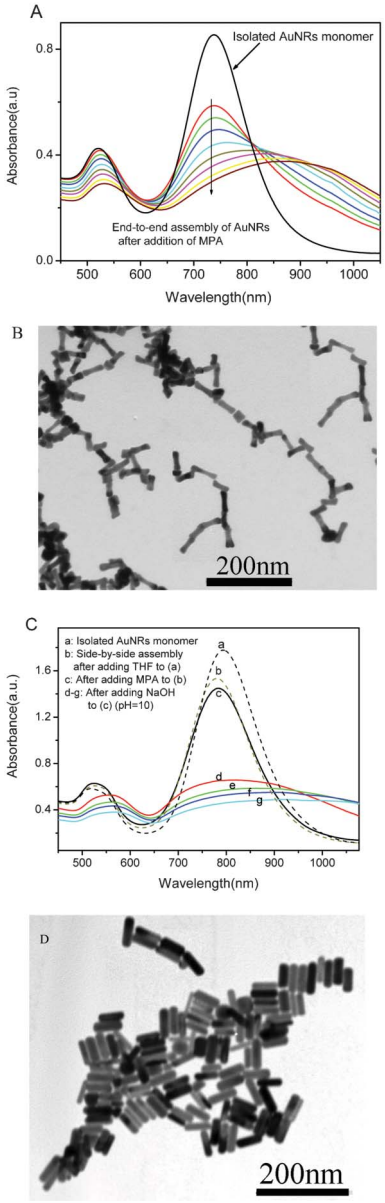

Fig. 4 Absorption spectra (A) and TEM image (B) of the end-to-end assembled AuNRs in the presence of MPA. (C) Absorption spectra of sample after adding MPA to the THF-induced side-by-side assembly AuNRs. (D) TEM image for the final product shows the linking of side-by-side assembled dimers and randomly aggregated side-by-side assembly.

SPR_L, whereas red-shifting of the longitudinal mode appears primarily for the end-to-end assembly of nanorods.[19,41,45–47] For this case, UV-Vis-NIR optical absorption measurement could be utilized to reveal the side-by-side assembly process of AuNRs from the spectra evolution, as shown in Fig. 2B. With increasing assembly time, significant blue shifting of SPR_L and slight red-shifting of SPR_T were observed, indicating the plasmons coupling of the two side-by-side neighboring AuNRs.[45,46,48–50] According to our best knowledge, it is the first report that only THF was applied to obtain side-by-side assembled AuNRs through such a simple and effective solution-phase method. TEM image of the isolated AuNRs was inserted up-right in Fig. 2B. Up-left inset of Fig. 2B presents HRTEM image of lattice spacing and SAED for the nanorod, indicating the single-crystalline nature of the obtained AuNRs.

Through a series of experiments, it is found that different amount of THF results in different assembly degree. When concentrated aqueous AuNRs colloid was dispersed in THF, the color of the solution of AuNRs turned quickly from red to gray-blue. The colloid colors for the AuNRs assembly with R_{TH} increasing from 1 : 10 to 1 : 5 are shown in Fig. 2C. Almost all AuNRs are side-by-side assembled in polymers with R_{TH} = 1 : 6, as indicated by the TEM image (Fig. 2D), and the intensity of SPR_L for this sample declines sharply with blue-shifting (Fig. 2E).

It is known that there are many factors influencing the yield and kinetics of side-by-side assembly of AuNRs besides the amount of THF, such as the concentration of CTAB and AuNRs, polar property of solvent, and keeping time of the as-prepared AuNRs. For the CTAB-stabilized AuNRs colloid kept at room temperature, obvious blue shifting and intensity damping of SPR_L were often detected due to surface atoms reconstruction at the end of AuNRs. Therefore, it is particularly worth noting that its quite different for the THF-induced side-by-side assembly between the as-prepared AuNRs (keeping at room temperature) and the ice-cold AuNRs. For example, when the AuNRs colloid was kept in refrigerator (5 °C) for ~30 min before adding THF (R_{TH} = 1 : 5, and R_{TH} = 1 : 8), the colloid color and optical spectra (see Fig. 3) were different from those of as-prepared AuNRs kept at room temperature with the same amount of THF (see Fig. 2). Thus, it is convincing that low temperature would limit the surface reconstruction of the AuNRs end facets, which in turn affect the steric stabilization and assembly kinetics.

AuNRs can also be assembled in solution *via* end-to-end orientation through binding proteins;[51,52] hydrophobic alkylthiols;[19,31] multicharged small molecules;[21,53] peptides[36,54] and thiolated polymers.[29,38,55] One of the small-molecule charged thiols named MPA is applied as a linker in our experiment. However, there is no obvious change for the sample after addition of MPA. With adjusting pH = 10, end-to-end assembly of AuNRs can proceed. In the optical spectra (see Fig. 4A), gradual decrease in intensity and broadening, and significant SPR_L red-shifting were observed, indicating an electromagnetic coupling in the SPR_L due to the end-to-end interacting of the AuNRs in solution. Correspondingly, TEM image for this assembly is shown in Fig. 4B. The end-to-end assembly of AuNRs has been postulated to occur through hydrogen-bond formation between carboxylic acids.[37] It is worth noting that a red-shift in the SPR_L is not, by itself, only a proof of end-to-end assembly. More random aggregation can also lead to this red-shift. As indicated by the stage 2 in Fig. 1, when 0.5 mM MPA was added to the THF-assembled AuNRs with pH = 10, strong decrease in intensity and broadening, and similar SPR_L shifting were observed, as shown in Fig. 4C. TEM image for the corresponding sample is shown in Fig. 4D,

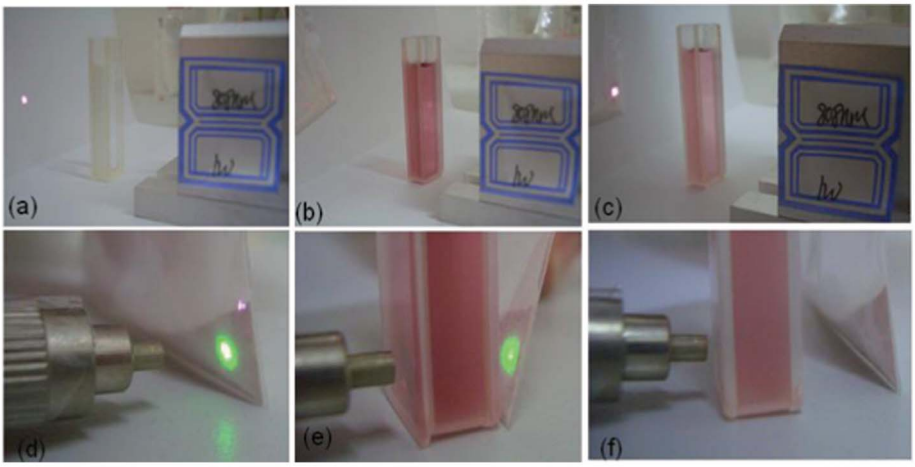

Fig. 5 Photographs showing the intensity of laser spot through water and AuNRs colloid with SPR_L at ~808 nm and 980 nm under the laser irradiation (luminescent material was used to provide the size and location of NIR laser spot), (a)–(c) laser wavelength 808 nm pass through water (a), AuNRs colloid with SPR_L 808 nm (b) and 980 nm (c). (d)–(f) Laser wavelength 980 nm, pass through luminescent material (d), AuNRs colloid with SPR_L 808 nm (e) and 980 nm (f).

indicating the aggregation (or linkage) of the side-by-side assembled AuNRs. The SPR_T in the optical spectra shows a small red-shifting, which is different from the result reported by Wang,[41] demonstrating a complex electromagnetic coupling in the short wavelength plasmon band due to linking and random aggregating of side-by-side assembled AuNR pairs. Based on the presented results, we can see that the assembly of AuNRs undergoes the transitions: side-by-side → bundles → end-to-end → chains (or aggregation).

Although some theoretical softwares were used to simulate SPR properties, and especially the coupling effect at the nanoscale gap of assembled nanostructures, theoretical modeling of small interparticle separation is challenging as the contribution of multipolar modes increases and the effect of the nearest neighbor interactions is unknown. Controllable assembly is now becoming robust enough to start producing structures that can be used to test (or improve) theoretical models. For the coupling SPR, although most reports utilize a red-shifted SPR_L as evidence of the end-to-end assembly, the exact nature of the red-shift and the degree of broadening often vary. In the applied science, the predetermined assemblies of AuNRs are promising in the fabrication of functional devices. These properties and possible applications rely on our ability to control the assembly, highly reproduce the assembly, understanding assembly process, surface functionalization along with well-defined arrangement are vital for this study.

For the tunable SPR_L of isolated AuNRs colloid or their aggregation in the NIR region, great interest has been attracted to the therapy in cancer research due to the high photothermal effect of NIR light. With the assistance of luminescent material and NIR lasers (such as 808 nm and 980 nm), we carried out the photothermal conversion of AuNRs colloids with SPR_L located at about 808 nm and 980 nm, respectively. Large amounts of experimental data show that AuNRs colloid selectively absorbed laser energy corresponding to their SPR_L wavelength from the intensity of laser spot (see Fig. 5). Compared with the deionized water, there are obvious increases in temperature for the AuNRs colloid after laser irradiation (not shown here). Further studies on the near-infrared plasmonic photothermal conversion of AuNRs and surface coating for biological compatibility are now being carried out in our lab, and some interesting results will be reported in a forthcoming paper.

Conclusions

In summary, we have demonstrated a new and facile way for side-by-side and end-to-end linked AuNRs controllable assembly using THF and MPA as linkers. It is the first report on utilizing THF to obtain side-by-side AuNRs dimers with a high yield with optimal volume ratio of THF : H_2O ranging from 1 : 8 to 1 : 6. The concentrations of CTAB and AuNRs, keeping time and temperature of the AuNRs colloid have an influence on the yield and kinetics of AuNRs assembly. Addition of MPA can induce end-to-end assembly of the as-formed side-by-side AuNRs pairs. This versatile and nonlithographic technique has potential for large scale fabrication of the next generation of inexpensive functional devices. Although the exact nature of the shifting and broadening of SPR_L is unknown, and the structure-property relationship varies, the SPR tunability of nanostructures shows great potential.

Acknowledgements

This study was financially supported by the National Natural Science Foundation of China (No. 11274173, 51032002, 61222403), the Fundamental Research Funds for the Central Universities and the Foundation of Graduate Innovation Center in Nanjing University of Aeronautics and

Astronautics, China (No. kfjj120125). TEM measurements in Nanjing University and Nanjing Medical University are also gratefully acknowledged.

Notes and references

1 W. L. Barnes, A. Dereux and T. W. Ebbesen, *Nature*, 2003, **424**, 824–830.
2 M. Quinten, *Optical Properties of Nanoparticle Systems: Mie and Beyond*, Wiley-VCH, 2011.
3 C. J. Murphy, A. M. Gole, J. W. Stone, P. N. Sisco, A. M. Alkilany, E. C. Goldsmith and S. C. Baxter, *Acc. Chem. Res.*, 2008, **41**, 1721–1730.
4 H. C. Li, C. X. Kan, Z. G. Yi, X. L. Ding, Y. L. Cao and J. J. Zhu, *J. Nanomater.*, 2010.
5 C. X. Kan, W. P. Cai, C. C. Li, G. H. Fu and L. D. Zhang, *J. Appl. Phys.*, 2004, **96**, 5727–5734.
6 J. Cao, E. K. Galbraith, T. Sun and K. T. V. Grattan, *IEEE Sens. J.*, 2012, **12**, 2355–2361.
7 P. Zijlstra, J. W. M. Chon and M. Gu, *Nature*, 2009, **459**, 410–413.
8 C. Novo, A. M. Funston and P. Mulvaney, *Nat. Nanotechnol.*, 2008, **3**, 598–602.
9 D. H. M. Dam, J. H. Lee, P. N. Sisco, D. T. Co, M. Zhang, M. R. Wasielewski and T. W. Odom, *ACS Nano*, 2012, **6**, 3318–3326.
10 E. M. Larsson, C. Langhammer, I. Zoric and B. Kasemo, *Science*, 2009, **326**, 1091–1094.
11 N. Bi, Y. H. Chen, H. B. Qi, X. Zheng, Y. Chen, X. Liao, H. Q. Zhang and Y. Tian, *Spectrochim. Acta, Part A*, 2012, **95**, 276–281.
12 E. Yasun, B. Gulbakan, I. Ocsoy, Q. Yuan, M. I. Shukoor, C. M. Li and W. H. Tan, *Anal. Chem.*, 2012, **84**, 6008–6015.
13 J. Wang, G. Z. Zhu, M. X. You, E. Q. Song, M. I. Shukoor, K. J. Zhang, M. B. Altman, Y. Chen, Z. Zhu, C. Z. Huang and W. H. Tan, *ACS Nano*, 2012, **6**, 5070–5077.
14 J. Choi, J. Yang, D. Bang, J. Park, J. S. Suh, Y. M. Huh and S. Haam, *Small*, 2012, **8**, 746–753.
15 J. S. Donner, S. A. Thompson, M. P. Kreuzer, G. Baffou and R. Quidant, *Nano Lett.*, 2012, **12**, 2107–2111.
16 H. C. Huang, K. Rege and J. J. Heys, *ACS Nano*, 2010, **4**, 2892–2900.
17 J. M. Liu, H. F. Wang and X. P. Yan, *Analyst*, 2011, **136**, 3904–3910.
18 J. Wang, P. Zhang, C. M. Li, Y. F. Li and C. Z. Huang, *Biosens. Bioelectron.*, 2012, **34**, 197–201.
19 Y. Wang, A. E. DePrince, S. K. Gray, X. M. Lin and M. Pelton, *J. Phys. Chem. Lett.*, 2010, **1**, 2692–2698.
20 N. Xiao and C. X. Yu, *Anal. Chem.*, 2010, **82**, 3659–3663.
21 H. W. Huang, C. T. Qu, X. Y. Liu, S. W. Huang, Z. J. Xu, Y. J. Zhu and P. K. Chu, *Chem. Commun.*, 2011, **47**, 6897–6899.
22 C. G. Wang, Y. Chen, T. T. Wang, Z. F. Ma and Z. M. Su, *Chem. Mater.*, 2007, **19**, 5809–5811.
23 A. R. Ferhan, L. H. Guo and D. H. Kim, *Langmuir*, 2010, **26**, 12433–12442.
24 M. Chirea, J. Borges, C. M. Pereira and A. F. Silva, *J. Phys. Chem. C*, 2010, **114**, 9478–9488.
25 A. Guerrero-Martinez, J. Perez-Juste, E. Carbo-Argibay, G. Tardajos and L. M. Liz-Marzan, *Angew. Chem., Int. Ed.*, 2009, **48**, 9484–9488.
26 F. Holzner, C. Kuemin, P. Paul, J. L. Hedrick, H. Wolf, N. D. Spencer, U. Duerig and A. W. Knoll, *Nano Lett.*, 2011, **11**, 3957–3962.
27 Y. Xie, S. M. Guo, Y. L. Ji, C. F. Guo, X. F. Liu, Z. Y. Chen, X. C. Wu and Q. Liu, *Langmuir*, 2011, **27**, 11394–11400.
28 C. Kuemin, L. Nowack, L. Bozano, N. D. Spencer and H. Wolf, *Adv. Funct. Mater.*, 2012, **22**, 702–708.
29 L. Kun, N. Zhihong, Z. Nana, L. Wei, M. Rubinstein and E. Kumacheva, *Science*, 2010, **329**, 197–200.
30 C. L. Zhang, K. P. Lv, H. P. Cong and S. H. Yu, *Small*, 2012, **8**, 648–653.
31 D. Nepal, K. Park and R. A. Vaia, *Small*, 2012, **8**, 1013–1020.
32 D. Fava, Z. Nie, M. A. Winnik and E. Kumacheva, *Adv. Mater.*, 2008, **20**, 4318–4322.
33 E. R. Zubarev, J. Xu, A. Sayyad and J. D. Gibson, *J. Am. Chem. Soc.*, 2006, **128**, 15098–15099.
34 Z. H. Nie, D. Fava, E. Kumacheva, S. Zou, G. C. Walker and M. Rubinstein, *Nat. Mater.*, 2007, **6**, 609–614.
35 K. K. Caswell, J. N. Wilson, U. H. F. Bunz and C. J. Murphy, *J. Am. Chem. Soc.*, 2003, **125**, 13914–13915.
36 X. G. Hu, W. L. Cheng, T. Wang, E. K. Wang and S. J. Dong, *Nanotechnology*, 2005, **16**, 2164–2169.
37 W. H. Ni, R. A. Mosquera, J. Perez-Juste and L. M. Liz-Marzan, *J. Phys. Chem. Lett.*, 2010, **1**, 1181–1185.
38 L. B. Zhong, X. Zhou, S. X. Bao, Y. F. Shi, Y. Wang, S. M. Hong, Y. C. Huang, X. Wang, Z. X. Xie and Q. Q. Zhang, *J. Mater. Chem.*, 2011, **21**, 14448–14455.
39 A. Abbas, L. M. Tian, R. Kattumenu, A. Halim and S. Singamaneni, *Chem. Commun.*, 2012, **48**, 1677–1679.
40 Z. N. Zhu, W. J. Liu, Z. T. Li, B. Han, Y. L. Zhou, Y. Gao and Z. Y. Tang, *ACS Nano*, 2012, **6**, 2326–2332.
41 Z. H. Sun, W. H. Ni, Z. Yang, X. S. Kou, L. Li and J. F. Wang, *Small*, 2008, **4**, 1287–1292.
42 X. C. Ye, L. H. Jin, H. Caglayan, J. Chen, G. Z. Xing, C. Zheng, D. N. Vicky, Y. J. Kang, N. Engheta, C. R. Kagan and C. B. Murray, *ACS Nano*, 2012, **6**, 2804–2817.
43 H. Nakashima, K. Furukawa, Y. Kashimura and K. Torimitsu, *Chem. Commun.*, **2007**, 1080–1082.
44 X. S. Kou, S. Z. Zhang, Z. Yang, C. K. Tsung, G. D. Stucky, L. D. Sun, J. F. Wang and C. H. Yan, *J. Am. Chem. Soc.*, 2007, **129**, 6402–6404.
45 A. M. Funston, C. Novo, T. J. Davis and P. Mulvaney, *Nano Lett.*, 2009, **9**, 1651–1658.
46 P. K. Jain and M. A. El-Sayed, *J. Phys. Chem. C*, 2008, **112**, 4954–4960.
47 P. K. Jain, S. Eustis and M. A. El-Sayed, *J. Phys. Chem. B*, 2006, **110**, 18243–18253.
48 L. Shao, K. C. Woo, H. J. Chen, Z. Jin, J. F. Wang and H. Q. Lin, *ACS Nano*, 2010, **4**, 3053–3062.
49 C. Tabor, D. Van Haute and M. A. El-Sayed, *ACS Nano*, 2009, **3**, 3670–3678.
50 S. L. Ke, C. X. Kan, B. Mo, B. Cong and J. J. Zhu, *Acta Phys.-Chim. Sin.*, 2012, **28**, 1275–1290.
51 Y. Y. Zhu, H. Kuang, L. G. Xu, W. Ma, C. F. Peng, Y. F. Hua, L. B. Wang and C. L. Xu, *J. Mater. Chem.*, 2012, **22**, 2387–2391.
52 L. B. Wang, Y. Y. Zhu, L. G. Xu, W. Chen, H. Kuang, L. Q. Liu, A. Agarwal, C. L. Xu and N. A. Kotov, *Angew. Chem., Int. Ed.*, 2010, **49**, 5472–5475.

53 L. Zhang, H. J. Chen, J. F. Wang, Y. A. F. Li, J. A. Wang, Y. Sang, S. J. Xiao, L. Zhan and C. Z. Huang, *Small*, 2010, **6**, 2001–2009.
54 W. W. He, S. Hou, X. B. Mao, X. C. Wu, Y. L. Ji, J. B. Liu, X. N. Hu, K. Zhang, C. X. Wang, Y. L. Yang and Q. Wang, *Chem. Commun.*, 2011, **47**, 5482–5484.
55 A. Lee, G. F. S. Andrade, A. Ahmed, M. L. Souza, N. Coombs, E. Tumarkin, K. Liu, R. Gordon, A. G. Brolo and E. Kurnacheva, *J. Am. Chem. Soc.*, 2011, **133**, 7563–7570.

